Journal of Physics: Conference Series **682** (2016) 012034 doi:10.1088/1742-6596/682/1/012034

Studying complex chemistries using PLASIMO's global model

PMJ Koelman, S Tadayon Mousavi, R Perillo, WAAD Graef, DB Mihailova and J van Dijk

Department of Applied Physics, Eindhoven University of Technology,
P.O. Box 513, 5600 MB Eindhoven, The Netherlands

E-mail: p.m.j.koelman@tue.nl

Abstract. The Plasimo simulation software is used to construct a Global Model of a CO_2 plasma. A DBD plasma between two coaxial cylinders is considered, which is driven by a triangular input power pulse. The plasma chemistry is studied during this power pulse and in the afterglow. The model consists of 71 species that interact in 3500 reactions. Preliminary results from the model are presented. The model has been validated by comparing its results with those presented in Kozák *et al.* (Plasma Sources Science and Technology **23**(4) p. 045004, 2014). A good qualitative agreement has been reached; potential sources of remaining discrepancies are extensively discussed.

1. Introduction

Numerical plasma simulations are a powerful tool for studying the characteristics and essential parameters of a plasma source and have enough predictive value to inspire the development of new plasma technologies. In modern plasma applications, such as plasma surface treatment, biomedical applications and environmental technologies, plasmas are typically created in a mixture of gases. As a consequence of the plasma activities, the filling gas is transformed into a myriad of excited atoms, molecules, radicals and various types of ions.

Two or three dimensional modeling of such a large number of plasma species results in a significant calculation time, from several days to weeks and even more. Global Models are only time resolved, and hence require less computational time than spatially resolved models. Therefore Global Models can be favourable tool to study the plasma processes for chemically complex plasmas.

The overall goal of this study is the efficient transformation of CO_2 in valuable fuels. This process starts with the dissociation of CO_2 in CO and $\frac{1}{2}O_2$, and the fuels are produced in subsequent steps. To that end we study the chemistry of a CO_2 plasma with particular interest in the vibrational levels of CO_2, which provide an energy efficient path for dissociation.

In this work we present a Global Model of CO_2, which is constructed using Plasimo simulation software [1, 5]. We use the same chemistry as Kozak *et al.* [2], who modeled a CO_2 plasma in a cylindrical concentric reactor using GlobalKin [3]. We make a detailed comparison between the results of our model and the results presented in [2], and the influence of the input power density on the CO_2 vibrational modes is studied.

2. The CO_2 Model

First the equations, which form the Global Model, will be introduced breefly. In the PhD thesis of W. Graef [5] an extended description of the Global Model can be found. Thereafter the model set-up and the used set of species and input data will be introduced.

2.1. Global Model

The Global Model solves the time evolution of the species densities n_s of the species s that occur in the plasma,

$$\frac{\mathrm{d}n_s}{\mathrm{d}t} = \sum_{i=1}^{j} (\beta_{i,s} - \alpha_{i,s}) R_i, \tag{1}$$

with j the number of reactions affecting n_s and R_i the rate of reaction i, which is given by:

$$R_i = k_i \prod_z n_z^{\alpha_{i,z}}. \tag{2}$$

Here k_i is the rate coefficient, n_z is the density of particle z and $\alpha_{i,z}$ and $\beta_{i,z}$ the numbers of particles of type z at the left and right hand sides of reaction i. The rate coefficient of reaction i follows from the cross sections using the relation:

$$k_i = \int_{E_{th}}^{\infty} v(\epsilon)\sigma_i(v) f(\epsilon)\, \mathrm{d}\epsilon, \tag{3}$$

with ϵ the energy, $v(\epsilon)$ the velocity of the electrons, $\sigma(v)_i$ the cross section of collision i, $f(\epsilon)$ the electron energy distribution function (eedf) and E_{th} the threshold energy of the collision. For the calculation of the eedf we use the free-ware Boltzmann solver BOLSIG+ [4].

Together with the particle balance, equation (1), the electron energy density balance is solved by:

$$\frac{\mathrm{d}E}{\mathrm{d}t} = \mathrm{P} - Q_{elas} - Q_{inelas}, \tag{4}$$

where P is the input power density, Q_{elas} the energy loss due to elastic collisions and Q_{inelas} the nett energy loss due to inelastic processes.

2.2. Model set-up

A dielectric barier discharge plasma between two coaxial cylinders is considered. The plasma has an inner radius of 11 mm and the outer radius at 13 mm. The length of the plasma cylinder is 90 mm.

Three different input power densities are used in the model: 1.06 10^7 W/m^3, 1.06 10^8 W/m^3 and 1.06 10^9 W/m^3. Figure 1 shows the shape of the input power pulse during the first 100 ns. The power rises in 15 ns towards the maximum value. Thereafter it lowers to 0 in the same period of time, resulting in a pulse duration of 30 ns. The total duration of the cycle is 2.9 10^5 ns.

The pressure is an input parameter which is set at 10^5 Pa. From the pressure the initial densities are calculated, resulting in a density of 1.9 10^{25} m^{-3} for CO_2. Other species in the ground state and the ions have a density of 1.9 10^{15} m^{-3}. The vibrational states are initially in Boltzmann equilibrium with the species in the ground state. The gas temperature is fixed at 300 K.

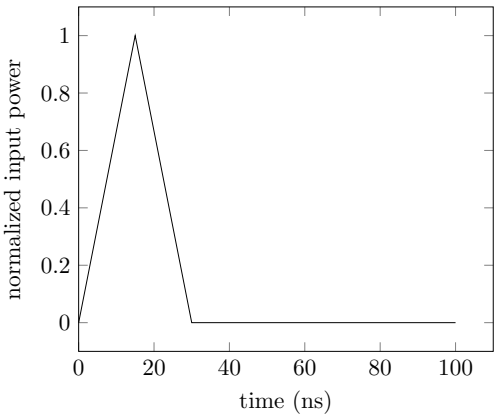

Figure 1. The shape of the input power as used in the model. Since the input power density in the model is one of the studied parameters, the normalized input power density is plotted. Here only the first 100 ns are depicted. The total duration of the cycle is $2.9\ 10^5$ ns.

Table 1. The list of species included in the model.

Neutrals	CO_2	CO	C_2O	C	C_2	O	O_2	O_3
Pos. ions	CO_2^+	CO_4^+	CO^+	$C_2O_2^+$	$C_2O_3^+$	$C_2O_4^+$		
	C^+	C_2^+	O^+	O_2^+	O_4^+			
Neg. ions	CO_3^-	CO_4^-	O^-	O_2^-	O_3^-	O_4^-		
Elec. excited	CO_2e_1	CO_2e_2	COe_1	COe_2	COe_3	COe_4	O_2e_1	O_2e_2
Vib. excited	CO_2v_a	CO_2v_b	CO_2v_c	CO_2v_d	$CO_2v_{1...21}$			
	$COv_{1...9}$	O_2v_1	O_2v_2	O_2v_3				

2.3. Chemistry

The model consists of 71 species, which form a set of 3500 reactions. The species are listed in table 1, where the excitation is denoted by e and v for the electronicly and vibrationally excited states respectively. Cross sections or rate coefficients are available in literature for most reactions in which neutrals or ions are involved. There is a lack of cross sections and rate coefficients for higher excited vibrational level. For that reason it is suggested in [2] to make use of scaling laws, which are based on reaction types. The reaction types that are considered in the model, are listed below. Two of the reaction types scaling laws are involved, which are described concisely.

- **Electron impact reactions**
  The cross sections of the vibrationally excited levels are obtained by scaling of the ground state species cross section by the so called Fridman approximation: scaling of the cross section by a shift in energy and a modification of the absolute value of the cross section.
- **Electron attachment and electron-ion recombination reactions**
- **Neutral-neutral reactions**
- **Ion-heavy particle reactions**
- **Vibrational energy transfer reactions**
  The rate coefficients of these reactions are scaled using the SSH (Schawartz, Slawski and Hertzfeld) theory [6]. The rate coefficients scale strongly with the vibrational mode number and the transition energy of the reaction.

At [2] an extensive description of the species and chemistry can be found.

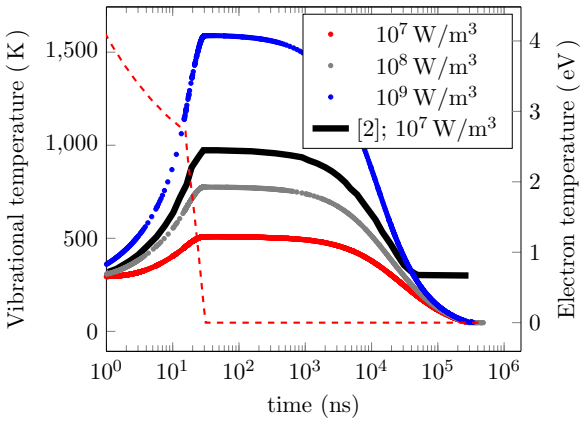

Figure 2. The vibrational temperature as a function of time at different values of the input power density, with logarithmic x-axis. The electron temperature is depicted using the red dashed line. The accompanying label is at the secondary y-axis at the right. Results of [2] are plotted as well for comparison.

3. Results and discussion

First, the results of the model will be analysed using the vibrational temperature of CO_2. Thereafter, the population of the vibrational levels will be the topic of discussion.

3.1. Vibrational temperature

Figure 2 shows the vibrational temperature as a function of time. During the power pulse, the first 30 ns, the vibrational temperature increases towards a maximum value. The electron temperature shoots up at the start of the pulse to a high value, followed by a decrease over time. The peak of the input power pulse can be recognized in the electron temperature by the elbow in the trend of the electron temperature at 15 ns. As the power pulse ends, the electron temperature decreases towards zero.

The rise in vibrational temperature stops at the moment when the electron temperature reaches zero. This result shows that the increase of vibrational temperature results from the electron impact collisions, which typically show an electron temperature dependence. The vibrational temperature starts to decrease significantly around 1000 ns. Within one millisecond the system is completely relaxed towards the equilibrium temperature.

The equilibrium temperature of the model is 0 K, while the vibrational temperature in a physical experiment would relax towards the temperature of the heavy particles. This difference in temperature is a result of omitting collisions of heavy particles which stimulate the population of vibrational levels from the ground state of CO_2.

Trends in the results are independent on the input power density. The input power density only influences the maximum vibrational temperature, which shows a non-linear dependence.

Agreement in the trend is observed when comparing the results with the results of [2]. There are, however, also differences between the results of the models. The vibrational temperature in the results of [2] reaches 950 K, which is significantly higher than the 500 K, which is observed for the same input power. Furthermore the system relaxes towards an equilibrium temperature of 300 K. The decay time of the vibrational temperature towards equilibrium is, with 0.1 ms, the same in both models.

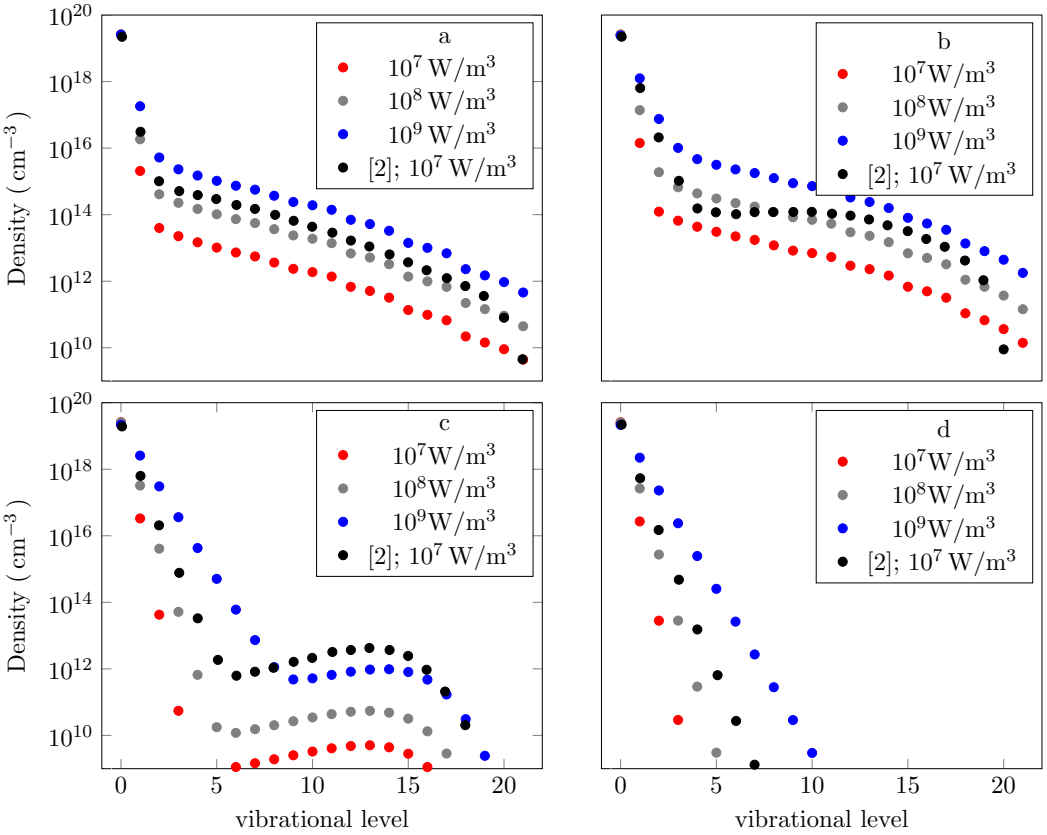

Figure 3. The distribution of vibrational levels after 6 ns , 30 ns , 100 ns and 1000 ns for the top left and right and bottom left and right respectively. The black markers show the results as obtained at [2]. The results are plotted in semi-logarithmic scale.

3.2. Vibrational level population

Figure 3 presents the population of the vibrational levels at four moments in time: at the start of the input power pulse 6 ns , at the end of the input power pulse 30 ns , at the early part of the afterglow 100 ns and further on during the afterglow, after 1000 ns .

The figures show the densities as a function of the vibrational level in logarithmic scale. During the start of the input power pulse the densities decrease linearly with the vibrational level, for vibrational levels above the first level. This trend is independent of the input power density. Increasing the input power density leads to an increased degree of ionization, while the electron temperature does not differ. This higher number of electrons does increase the rate for electron impact collisions, which is a linear dependence (cf. equation (2)).

At the end of the power pulse (at 30 ns , figure b) the distribution of the vibrational level densities do not differ significantly from the results at 6 ns , besides an increase in the densities. At this time the population of the vibrational levels increases, while the gradient remains unchanged.

In the early stage of the afterglow the results show that the vibrational levels, up to level 4-7, the densities exhibit a Boltzmann distribution. For the higher vibrational levels a more salient region can be defined. Species within this region show an inverse trend: increasing population for increasing vibrational level. This region of inverse trend reaches up to the 14$^{\text{th}}$ vibrational level. Further on during the afterglow, the results manifest a Boltzmann distribution.

During the afterglow the input power does show an influence on the scaling. During the early

part of the afterglow, when the region of inverse scaling is present, the number of vibrational levels in this region are dependent on the input power density. For low input power densities the number of species forming this region is larger than for high input power densities.

The trends of [2] are all in close agreement with the results which are presented here. The difference in absolute densities is likely to be a result of the differences in the models. In the analysis of figure 2 is pointed out that it is likely that the chemistry still needs a modification to balance the chemistry in the afterglow towards a Boltzmann equilibrium at 300 K . It is hard to oversee the consequence of such an addition. It is however well possible that such an addition would stimulate the population of the vibrational levels and that the results will be in even closer agreement.

4. Conclusion and outlook

The Plasimo simulation software is used to construct a Global Model of CO_2 plasma. A dielectric barier discharge plasma is considered, situated between two coaxial cylinders. The plasma, consisting of 71 species which form 3500 reactions, is driven by a triangular shaped power pulse. The vibrational levels of the plasma are studied during the power pulse and the afterglow.

The preliminary results show a trend in vibrational temperature which is independent of the input power density. The population of the vibrational levels show a similar scaling during the time the input power pulse is active. During the early stage of the afterglow there is, however, an input power density dependence observed. A region is defined for which the trend of the vibrational level population exhibits an inverse trend. The size of this region is input power density dependent, with an increased number of vibrational levels within this region for decreased input power density. Further on in the afterglow the temperature dependence in the scaling is not present anymore.

The relaxation of the vibrational temperature in the model is towards 0 K . This is due to the absence of reactions which populate the vibrational levels from the CO_2 ground state via heavy-heavy particle collisions. Extending the chemistry with these reactions is needed.

The scaling in the presented results is in close agreement with results from literature. The major difference between the results of the model and literature is in the absolute value for the vibrational densities, for the same input power density.

In the near future the aim is to complete the chemistry so that the system reaches a Boltzmann distribution at the heavy particle temperature. When the model is further validated based on results of other models, the chemistry will be expanded by adding more vibrational levels of O_2.

Acknowledgements

This research is supported by the Dutch Technology Foundation STW, which is part of the Netherlands Organisation for Scientific Research (NWO), and which is partly funded by the Ministry of Economic Affairs.

References

[1] van Dijk J, Peerenboom K, Jimenez M, Mihailova D and van der Mullen J 2009 *Journal of Physics D: Applied Physics* **42** 194012 URL `http://stacks.iop.org/0022-3727/42/i=19/a=194012`

[2] Kozk T and Bogaerts A 2014 *Plasma Sources Science and Technology* **23** 045004 URL `http://stacks.iop.org/0963-0252/23/i=4/a=045004`

[3] Dorai R 2002 *Modelling of atmospheric pressure plasma processing of gasses and surfaces* Ph.D. thesis University of Illinois at Urban-Champaign

[4] Hagelaar G J M and Pitchford L C 2005 *Plasma Sources Science and Technology* **14** 722 URL `http://stacks.iop.org/0963-0252/14/i=4/a=011`

[5] Graef W A A D 2012 *Zero-dimensional models for plasma chemistry* Ph.D. thesis Eindhoven University of Technology, The Netherlands

[6] Fridman A 2008 *Plasma chemistry* (Cambridge New York: Cambridge University Press) ISBN 9780521847353